JOURNAL OF SOLID STATE CHEMISTRY 113, 193–204 (1994)

High-Resolution Electron Microscopic Study of $Ba_7Sc_6Al_2O_{19}$ and Related Phases

R. V. Shpanchenko,[1] L. Nistor,[2] G. Van Tendeloo,[3] and S. Amelinckx

University of Antwerp (RUCA), Groenenborgerlaan 171, 2020 Antwerp, Belgium

and

E. V. Antipov and L. M. Kovba

Chemical Department, Moscow State University, 119899 Moscow, Russia

Received November 29, 1993; accepted February 9, 1994

It is shown that the crystal structures of the compound $Ba_7Sc_6Al_2O_{19}$ and of related structures which belong to the class of hexagonal perovskites can be interpreted as mixed-layer structures consisting of the intergrowth of structural blocks (or lamellae) of β-Ba_2ScAlO_5 and $Ba_3Sc_4O_9$, two other hexagonal perovskites. The block sequences have been imaged directly by means of high-resolution electron microscopy. The characteristic geometrical features of the structural blocks allow unambiguous identification of the different sequences. The image interpretation was confirmed by computer-simulated images. The structures can alternatively be considered as interface modulated structures derived from a cubic stacking of close-packed BaO_3 layers in which periodic stacking faults and twin boundaries are introduced. These interfaces are stabilized by B cations.

1. INTRODUCTION

Structural studies of increasingly more complicated layered inorganic phases have recently led to the discovery of several homologous series of intergrowth structures (1–7). In the structures of such phases, two (or more) types of structural blocks (or lamellae) occur in periodic sequences. The lamellae themselves must be possible building units of simpler structures. Historically the barium ferrites (1) and the chlorites (8) were among the first extensive homologous series to be recognized as "mixed-layer" structures or intergrowth structures.

The terminology used in the description of such structures is somewhat confusing. In this paper "intergrowth structures" are phases formed by the stacking of at least two types of lamellae U and V, where each type of lamella when periodically repeated as $\cdots UUU \cdots$ or $\cdots VVV \cdots$ generates an existing simpler structure. The structures U_n and V_n are the terminal members of the homologous series of intergrowth structures: $U_nV_mU_pV_q \cdots U_rV_s$. These different phases can be considered as belonging to a pseudo-binary system U-V.

It is clear that such intergrowth structures can only occur when a number of conditions are satisfied, the most fundamental one being that epitaxy must be possible along the contact plane between the two types of structural blocks. This will often be the case for two structures based on close-packed layers of the same anions or of the same combination of anions and cations, e.g., layers consisting of oxygen, sulfur, selenium, ..., or BaO_3, LaO_3, ... Many of the well-known intergrowth structures are indeed based on such close-packed layers, as, for instance, in the barium ferrites (1), where the layers are oxygen and BaO_3, and in $As_2Te_3(GeTe)_n$ (2), where the layers are tellurium. A number of homologous series of hexagonal perovskites can be considered as intergrowth structures. The best known examples are compounds with a general formula $A_nB_{n-1}O_{3n}$ (9–12). In these compounds the intergrowth occurs between blocks made up from and limited by close-packed layers. The deformability of such layers is much smaller than that of layers with square symmetry (like in the high-T_c superconductors), and as a result the conditions for epitaxy are much more stringent. In order to fulfill the matching conditions as accurately as possible, isomorphous substitutions of cations with different ionic radii may sometimes be required.

Close packing is not a necessary condition, however. In the various homologous series of high-T_c superconducting layered cuprates the constituent lamellae are parallel to

[1] On leave from the Chemical Department, Moscow State University, 119899 Moscow, Russia.

[2] On leave from the Institute of Atomic Physics I.F.T.M., P.O. Box Mg. 6, Bucharest, Romania.

[3] To whom correspondence should be addressed.

0022-4596/94 $6.00

(001) layers with square or orthorhombic symmetry. For instance, in the bismuth-based series $Bi_2Sr_2Ca_{n-1}Cu_nO_{2n+4}$ (3, 4) the structures consist of a perovskite-like block of variable thickness, i.e., containing a variable number of CuO_2 layers and calcium layers in lamellae of the type $\cdots SrO-(CuO_2-Ca)_n-CuO_2-SrO\cdots$ and of blocks of Bi_2O_2. The condition for epitaxy is not well satisfied in this case, the lattice parameter for Bi_2O_2 being significantly smaller than that of the perovskite block, which is essentially determined by the Cu–O bond length in the CuO_2 layers. Nevertheless intergrowth structures are formed, but the structures are deformation modulated. This modulation has been attributed primarily to the lattice mismatch between the two types of structural fragments and to the associated strain.

In some cases intergrowth structures occur even though the lattices of the two lamellae have a different rotation symmetry and only fit along one lattice direction in the layer plane. This is, for instance, the case in the MTS_3 compounds (13) (M = Pb, Sn; T = Nb, Ta). MS lamellae with square symmetry (deformed sodium chloride structure) alternate with TS_2 lamellae with hexagonal symmetry (NbS_2 structure).

Intergrowth structures usually contain long sequences which are not strictly periodic; therefore their study by means of X-ray diffraction can only provide some average structure. On the other hand high-resolution electron microscopy allows the direct imaging of very long or even nonperiodic sequences of layers.

The structure of a recently discovered complex oxide $Ba_7Sc_6Al_2O_{19}$ (14) was interpreted in terms of the regular alternation of structural blocks of β-Ba_2ScAlO_5 (15) and $Ba_3Sc_4O_9$ (16) stacked along the c-axis of the hexagonal cell. The ideal matching of these elementary structural blocks in $Ba_7Sc_6Al_2O_{19}$ suggests the possibility of the existence of a series of compounds with different ratios of the elementary blocks. In order to verify this assumption $Ba_7Sc_6Al_2O_{19}$ and related structures were studied by the combined use of X-ray and electron diffraction and high-resolution electron microscopy.

2. EXPERIMENTAL

The $Ba_7Sc_6Al_2O_{19}$ compound was prepared by solid-state reaction of $BaCO_3$, Sc_2O_3, and Al_2O_3 previously dried at 400°C. Starting materials were weighted and mixed, and after grinding the powder was pressed into pellets. The pellets were heated in air at 1250°C for 50 hr. The X-ray phase analysis (FG-552 Guinier camera, Cu$K\alpha_1$ radiation) was used for sample characterization.

The high-resolution electron microscopy observations were made on freshly powdered samples dispersed on copper grids covered with holey carbon film. Observations were carried out using a 400-kV microscope with a point resolution of 0.17 nm. The electron diffraction experiments, exploring reciprocal space, were performed using a 100-kV instrument.

3. THE PARENT STRUCTURES

The series of compounds under discussion incorporates subunit cell elements of two simpler structures, β-Ba_2ScAlO_5 and $Ba_3Sc_4O_9$; we shall call them the parent structures. Both are hexagonal perovskite-like structures. We shall focus attention only on the structural features of these compounds which are required for a proper understanding of the high-resolution electron microscopic observations.

3.1. The Crystal Structure of β-Ba_2ScAlO_5

The structure is represented by means of the coordination polyhedra for B cations in Fig. 1a. This structure is based on a framework of the 8H $(cchc)_2$ close packing of BaO_3 layers, its space group being $P6_3/mmc$. The same structure is realized in Ba_2InAlO_5 (17). Oxygen vacancies (required by stoichiometry) are orderly located in the "h"-type lamellae. This ordering leads to the formation of BaO layers creating tetrahedrally coordinated sites for the Al atoms. The pairs of tetrahedra have their common apex in the BaO layer and have their bases in the adjacent BaO_3 layers. In the BaO layer each Ba ion is surrounded by three oxygen ions and vice versa. As a result the cubically stacked layers on both sides of the BaO layers are in a twin relationship. Similar coordination for Ba atoms was found in the Ba_4OCl_6 structure (18). Sc atoms occupy the centers of oxygen octahedra. The resulting structure can thus be considered a polysynthetically twinned crystal. This is especially evident in a view along the close-packed rows (Fig. 1b). We can devide the structure into two arbitrarily chosen blocks W and W'. The most convenient choice, but by no means the only one, is one in which W and W' both have a symmetry plane. The blocks W and W' are moreover related by a 180° rotation about the c-axis. Consequently, the block sequence becomes $\cdots$/WW'WW'/$\cdots$, where the pair WW' corresponds to the unit cell.

3.2. The Crystal Structure of $Ba_3Sc_4O_9$

The crystal structure of this oxide is represented in Fig. 2a. It is derived from the 9R $(cch)_3$ sequence of close-packed BaO_3 layers and has $R\bar{3}m$ symmetry, but it is not the usual close packing realized in rhombohedral structures. The actual sequence results from the 12R $(cchh)_3$ sequence by removing every second h-type BaO_3 layer. The final structure then contains blocks of the initial close packing and also blocks, where two successive BaO_3 layers are stacked vertically. With such a BaO_3 layer stacking

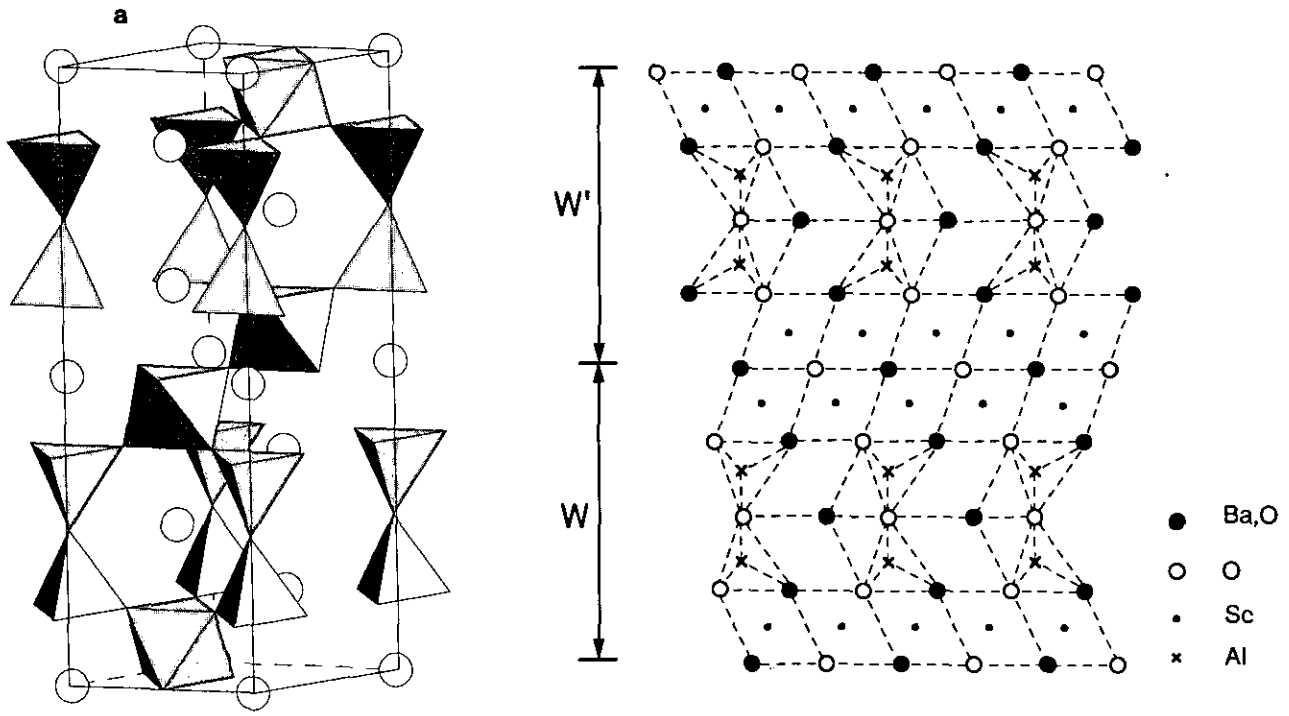

FIG. 1. Crystal structure of β-Ba_2ScAlO_5: (a) in terms of coordination polyhedra of *B* cations, and (b) viewed along the closed-packed rows.

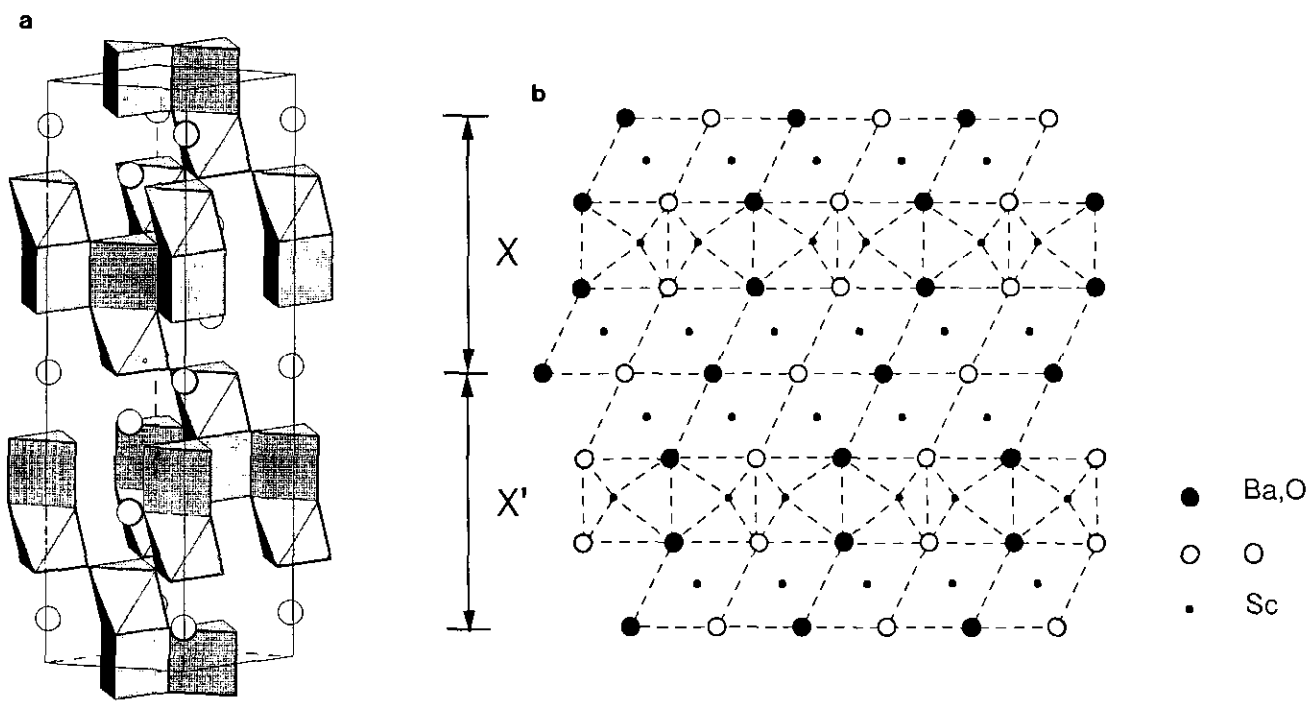

FIG. 2. Crystal structure of $Ba_3Sc_4O_9$: (a) in terms of coordination polyhedra of *B* cations, and (b) viewed along the closed-packed rows.

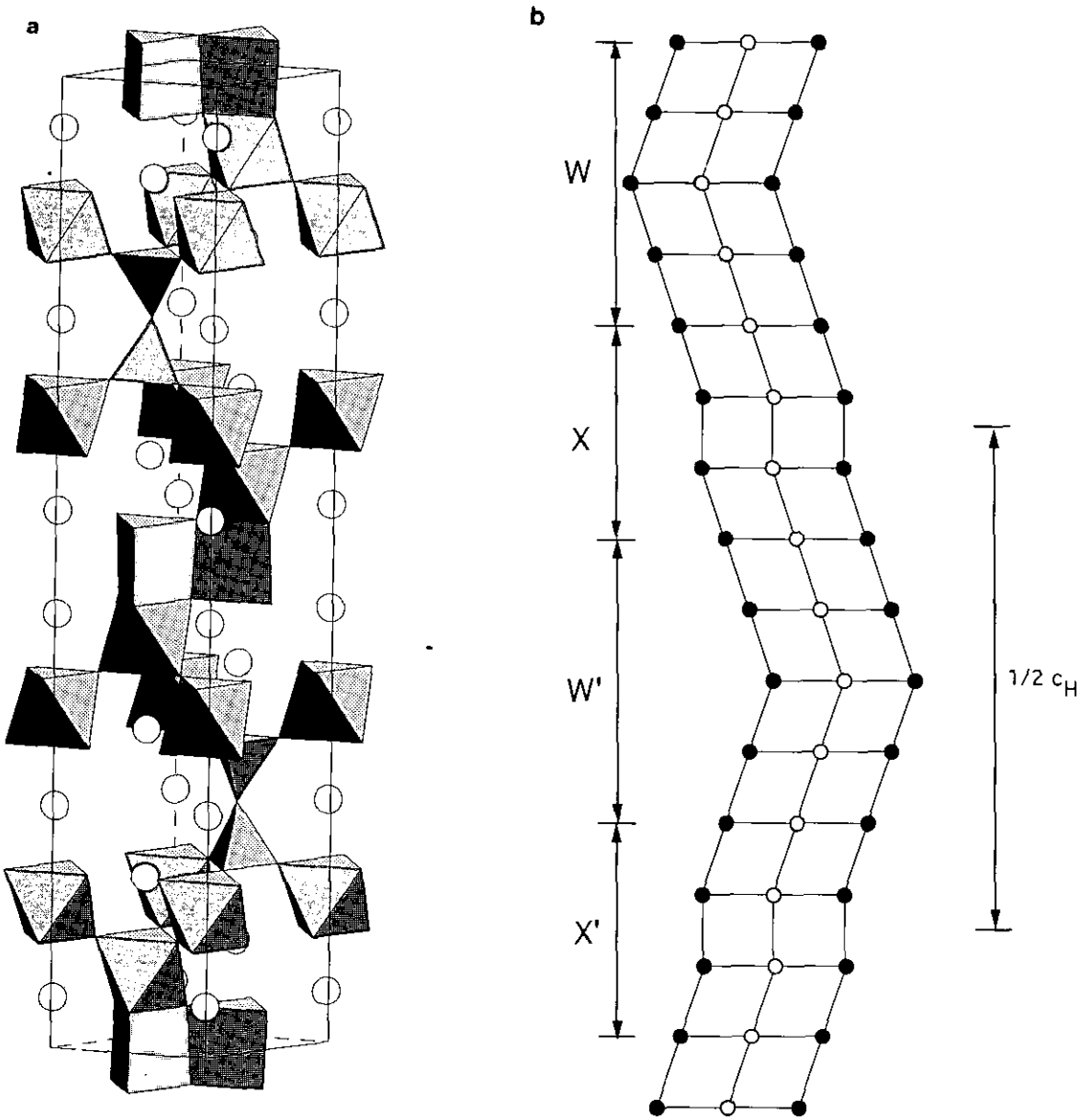

FIG. 3. Crystal structure of $Ba_7Sc_6Al_2O_{19}$: (a) in terms of coordination polyhedra of *B* cations, and (b) highly simplified view along the closed-packed rows.

two of the three face-sharing octahedra (which are present in the $(cchh)_3$ sequence) are transformed into trigonal prisms also occupied by Sc atoms. The number density of trigonal prismatic interstices is twice as large as that of the octahedral interstices between normally stacked layers. Therefore this layer has the composition Sc_2. It is easy to see the relation of this structure with the usual hexagonal perovskites ABO_3 if we write the formula as $Ba_3\square Sc_4O_9\square_3$. Crystal structures of other compounds $Ba_3R_4O_9$ (R = rare earth) are described in (19).

The succession of layers as viewed along the close-packed direction is represented in Fig. 2b. Note the small lateral shift of the oblique sequences of dots at the level of the trigonal prismatic layer. In this case the structure, which is rhombohedral, can be devided into three topologically equivalent blocks. The complete structure is then represented by the block sequence $\cdots/XXX/\cdots\cdot$. A topologically equivalent structure is generated by the sequence of blocks $\cdots/X'X'X'/\cdots$, where X' results from X by a rotation over 180° about the *c*-axis.

3.3. *The Crystal Structure of* $Ba_7Sc_6Al_2O_{19}$

The crystal structure of $Ba_7Sc_6Al_2O_{19}$, as deduced by X-ray diffraction, is shown in Fig. 3a. It is based on the

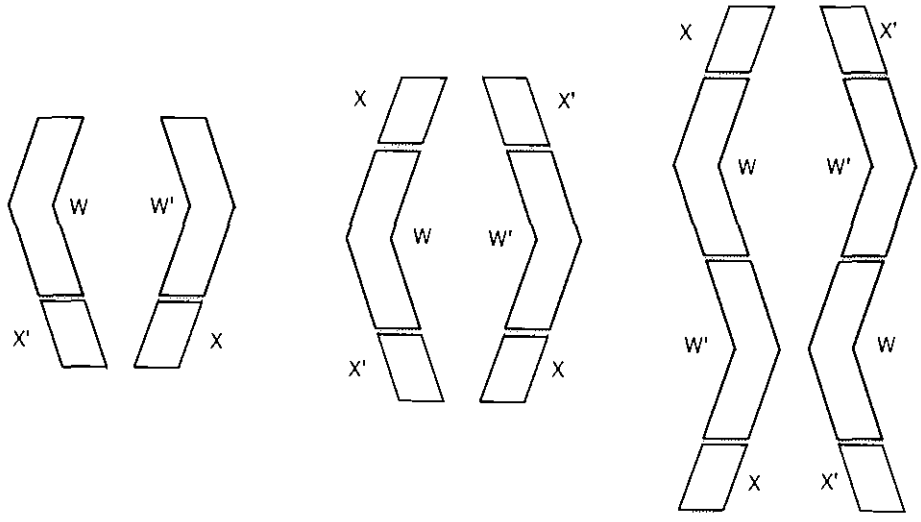

FIG. 4. Allowed stacking modes of W- and X-type blocks.

14H $(ccchccc)_2$ sequence of BaO_3 layers. It can clearly be dissected in blocks, as is particularly evident if this structure is represented as viewed along the close-packed direction and compared with similar views of the parent structures (Fig. 3b). It then becomes evident that the structure can be generated by the stacking of blocks of the type X and W in the succession $\cdots$/WXW'X'/$\cdots$, where W and W' differ by 180° in orientation, as well as X and X'. The composition of the W(W') blocks is $Ba_4Sc_2Al_2O_{10}$, and that of the X(X') blocks is $Ba_3Sc_4O_9$. Note that the considered blocks are separately charge balanced.

$Ba_7Sc_6Al_2O_{19}$ is the simplest example of an intergrowth structure of β-Ba_2ScAlO_5 and $Ba_3Sc_4O_9$ blocks; the composition is given by $2 \times \beta$-$Ba_2ScAlO_5 + Ba_3Sc_4O_9$. This 2 : 1 ratio is determined by the presence of a characteristic structural fragment containing two corner-sharing tetrahedra.

4. THE BUILDING PRINCIPLES OF INTERGROWTH STRUCTURES

The example of $Ba_7Sc_6Al_2O_{19}$ mentioned above the description of its structure in terms of two building blocks X and W indicated in Fig. 3b suggest that more complicated sequences of such blocks may occur, especially if we take into account the ideal matching of the basic W(W') and X(X') structural fragments, which are both limited on both sides by BaO_3 layers having the same lattice dimensions in the basal plane. In the intergrowth structures these limiting layers are common to both structural fragments.

It is possible to generalize this prototypic structure $\cdots$/WXW'X'/$\cdots$, in which X and W blocks are equally abundant, in two ways:

(I) by increasing the relative abundancy of X-type blocks;

(II) by increasing the relative abundancy of W-type blocks.

In this way two principal homologous series are created. These procedures cannot be applied in an arbitrary way, however. Obvious geometrical constraints impose restrictions which can be formulated as stacking rules.

Also it is found empirically that certain situations, although geometrically possible, have not been observed. This is, for instance, the case for the sequences $\cdots$/WWW/$\cdots$ or $\cdots$/W'W'W'/$\cdots$, presumably because this would create additional layers of face-sharing octahedra and consequently produce different structures.

The following rules apply to the first homologous series (I).

(i) W and W' blocks are always isolated, and their number in one repeat period is always even;

(ii) X (or X') blocks can occur in a succession of the same blocks;

(iii) W and W' blocks should alternate in a sequence;

(iv) sequences of X or X' blocks should always be separated by a W or a W' block;

(v) the sense of inclination of X (or X') blocks in a diagram such as Fig. 3b should always be the same as that of the W (or W') block to which it is attached, otherwise additional face-sharing octahedra would be formed.

Allowed stacking modes are shown schematically in Fig. 4.

Similar rules apply to the second homologous series (II).

(i) X (or X′) blocks are isolated, and their number in the repeat period is always even;

(ii) in a succession of W-type blocks W and W′ blocks alternate;

(iii) sequences of W-type blocks should be separated by X (or X′) blocks.

Rules (iv) and (v) of the above mentioned rules still apply.

The stacking of the blocks, together with the symmetry of the blocks themselves, obviously determines the symmetry and space group of the sequence. Again some simple rules are of help for determining the overall symmetry of the sequence.

(i) The presence of an X block causes a relative translation over $\frac{1}{3}$, $\frac{2}{3}$, 0 along the $[11\bar{2}0]$ direction, whereas the presence of an X′ block causes a relative translation in the opposite sense along the same direction.

(ii) The insertion of a W block changes a sequence of X blocks into a sequence of X′ blocks, whereas a W′ block has the opposite effect. The presence of a W block causes a mirror operation but no relative translation.

(iii) If the number of X blocks is equal to the number of X′ blocks in the repeat the overall symmetry of the resulting sequence is hexagonal, whereas if these numbers are unequal the overall symmetry is rhombohedral. In a hexagonal description the c_H parameter is then three times the repeat of the sequence.

(iv) The space group of a given sequence depends not only on the relative abundance of the two blocks but also on their specific sequence.

Applying these rules to the sequence $\cdots$/WXW′X′/$\cdots$, the space group is found to be $P6_3/mmc$ by considering the "local" symmetry of the blocks as well as their stacking.

We now discuss a number of examples of the two series of homologous compounds so far considered. We first note that the $\cdots$/WXW′X′/$\cdots$ structure with composition $Ba_7Sc_6Al_2O_{19}$ can be considered as a member of both series, which are produced by adding the appropriate number of W- or X-type blocks.

4.1. *Homologous Series (I)*

Sequences can be considered to obey the general stacking

$$\cdots/(\mathrm{X}\cdots\mathrm{X})_p\mathrm{W}(\mathrm{X}'\cdots\mathrm{X}')\mathrm{qW}'/\cdots=\cdots/\mathrm{X}_p\mathrm{WX}'_q\mathrm{W}'/\cdots$$

and have the chemical composition

$$Ba_{3n+8}Sc_{4n+4}Al_4O_{9n+20}, \quad \text{where } n = p + q.$$

If $p = q$ the structure is hexagonal, whereas it is rhombohedral if $p \neq q$. The observed examples belonging to this series are:

(1) The $\cdots$/XWX′X′W′/XWX′X′W′/$\cdots$ sequence corresponds to the composition

$$3 \times Ba_3Sc_4O_9 + 2 \times Ba_4Sc_2Al_2O_{10} = Ba_{17}Sc_{16}Al_4O_{47}.$$

Using the symmetry rules we obtain a rhombohedral symmetry since $p \neq q$. The unit cell includes three repeat periods of the sequence.

(2a) The second sequence in this series is $\cdots$/XXW X′X′W′/XXWX′X′W′/$\cdots$, corresponding to the composition

$$4 \times Ba_3Sc_4O_9 + 2 \times Ba_4Sc_2Al_2O_{10} = Ba_{20}Sc_{20}Al_4O_{56} \text{ (or } Ba_5Sc_5AlO_{14}).$$

The symmetry of this sequence is hexagonal.

(2b) The same composition $Ba_5Sc_5AlO_{14}$ can be obtained by another sequence: $\cdots$/XWX′X′X′W′/XWX′ X′X′W′/$\cdots$. This sequence has rhombohedral symmetry with three repeats in its unit cell.

The two sequences just mentioned have the same composition; $Ba_5Sc_5AlO_{14}$ can thus occur in two polytypic forms. No evidence has yet been found for the strongly asymmetric sequence that would be present in the second sequence. For energetic reasons the twin interfaces associated with the W-type blocks tend to be as far apart as the composition allows. The more symmetric sequence, which is the observed one, is therefore the more probable one.

This remark gives rise to an additional empirical rule: the length of X and X′ sequences, i.e., p and q, can differ only by one unit at most. Note that regular sequences where p (or q) > 3 occur rather rarely. This observation reflects also the fact that such long sequences correspond to very weak minima in free energy (i.e., a factor of thermodynamic stability).

Also, sequences containing more then two W-type blocks are conceivable as, for instance, $\cdots$/XWX′X′W′ XXWX′W′/$\cdots$. The symmetry of such sequences can be deduced from the rules presented above. However, a simple generalization can be formulated only for sequences containing two W blocks.

We now consider the pseudo-binary cut Ba_2ScAlO_5–$Ba_7Sc_6Al_2O_{19}$. The geometrical rules for this series of compounds are considered below.

4.2. *Homologous Series (II)*

The second homologous series is formed when inserting progressively W-type blocks in the $\cdots$/XWX′W′/$\cdots$ sequence of the $Ba_7Sc_6Al_2O_{19}$ structure. A general formula for the stacking sequence of this type is of the form

$$\cdots \mathrm{W}^*_p \cdots \mathrm{X}^* \cdots \mathrm{X}^*_q \cdots \mathrm{X}^* \cdots .$$

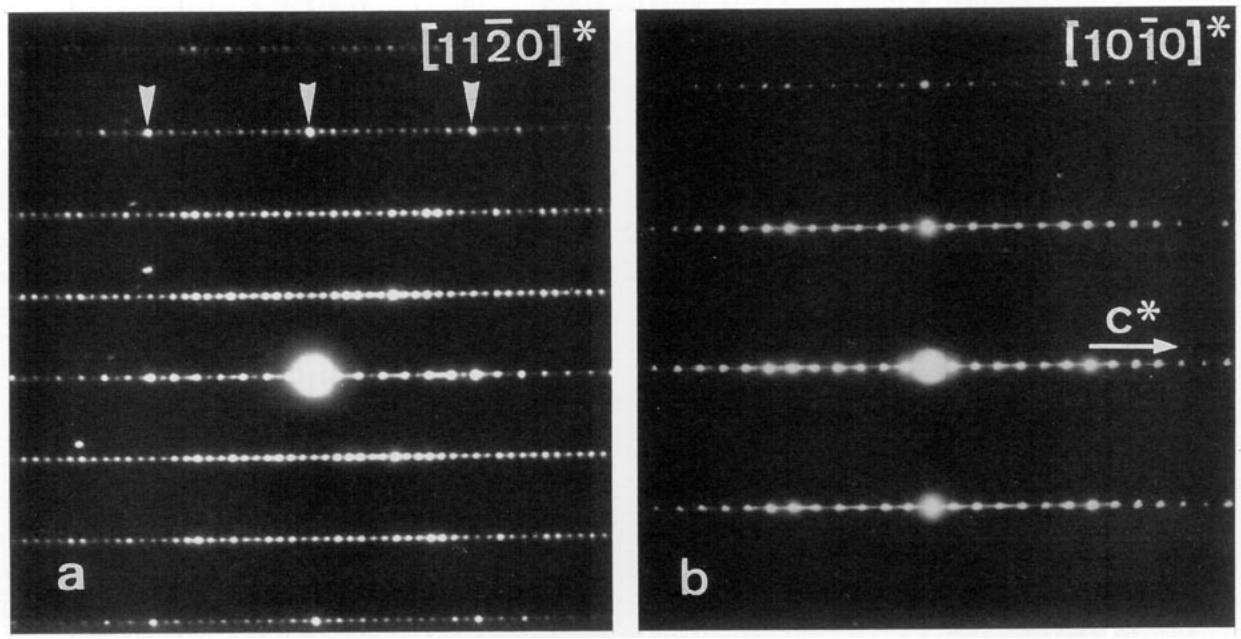

FIG. 5. Electron diffraction patterns of $Ba_7Sc_6Al_2O_{19}$: (a) [11$\bar{2}$0]* zone; (b) [10$\bar{1}$0]* zone.

In this formula $\cdots W_p^* \cdots$ (or $\cdots W_q^* \cdots$) means the alternation of W and W′ blocks. The type of X* block (X or X′) will depend on the parity of p and q, i.e., on which of the blocks W or W′ terminates the $\cdots WW' \cdots$ sequence.

As examples, we consider two members of this homologous series:

(1) The sequence $\cdots$/XWW′/XWW′/$\cdots$ corresponds to the composition

$$1 \times Ba_3Sc_4O_9 + 2 \times Ba_4Sc_2Al_2O_{10} = Ba_{11}Sc_8Al_4O_{29}.$$

The symmetry of this sequence is rhombohedral; therefore three repeat sequences correspond to the unit cell.

(2) For the block sequence $\cdots$/XWW′WX′W′WW′/$\cdots$ the composition would be

$$2 \times Ba_3Sc_4O_9 + 6 \times Ba_4Sc_2Al_2O_{10} = Ba_{30}Sc_{20}Al_{12}O_{78} \text{ (or } Ba_{15}Sc_{10}Al_6O_{39}).$$

The symmetry is hexagonal.

Of course, complex sequences including more than two X blocks may exist. However, we do not consider all possible cases in this paper. For the homologous series under consideration we can write a general formula for the composition:

$$Ba_{2n+3}Sc_{n+4}Al_nO_{5n+9}, \quad \text{where } n = p + q.$$

5. ELECTRON DIFFRACTION PATTERNS

The electron diffraction patterns of the prototype compound $\cdots WXW'X' \cdots$ along the [11$\bar{2}$0]* and [10$\bar{1}$0]* zones are reproduced in Fig. 5. Since the structure can to a good approximation be considered as being polysynthetically twinned on (0001), in particular when viewed along the [11$\bar{2}$0]* zone, the diffraction pattern exhibits the characteristic features due to this type of crystal texture, as described in (20–23).

In the third dense row of spots (Fig. 5a) the most intense spots correspond to $l = 14$; the corresponding interplanar distance is equal to the separation beteen successive BaO_3 layers, i.e., 2.51 Å. This feature is in accordance with the fact that the hexagonal cell contains 14 BaO_3 layers.

The twinned character leads to the presence of a twofold screw axis along the c direction. This is reflected in the diffraction pattern by the diffraction condition: 000l is only present for l = even. This can be concluded from the [10$\bar{1}$0]* zone diffraction pattern. The presence in the [11$\bar{2}$0]* zone pattern of weak spots with l = odd must be attributed to double diffraction out of noncentral rows.

The twinned character is further reflected in the inten-

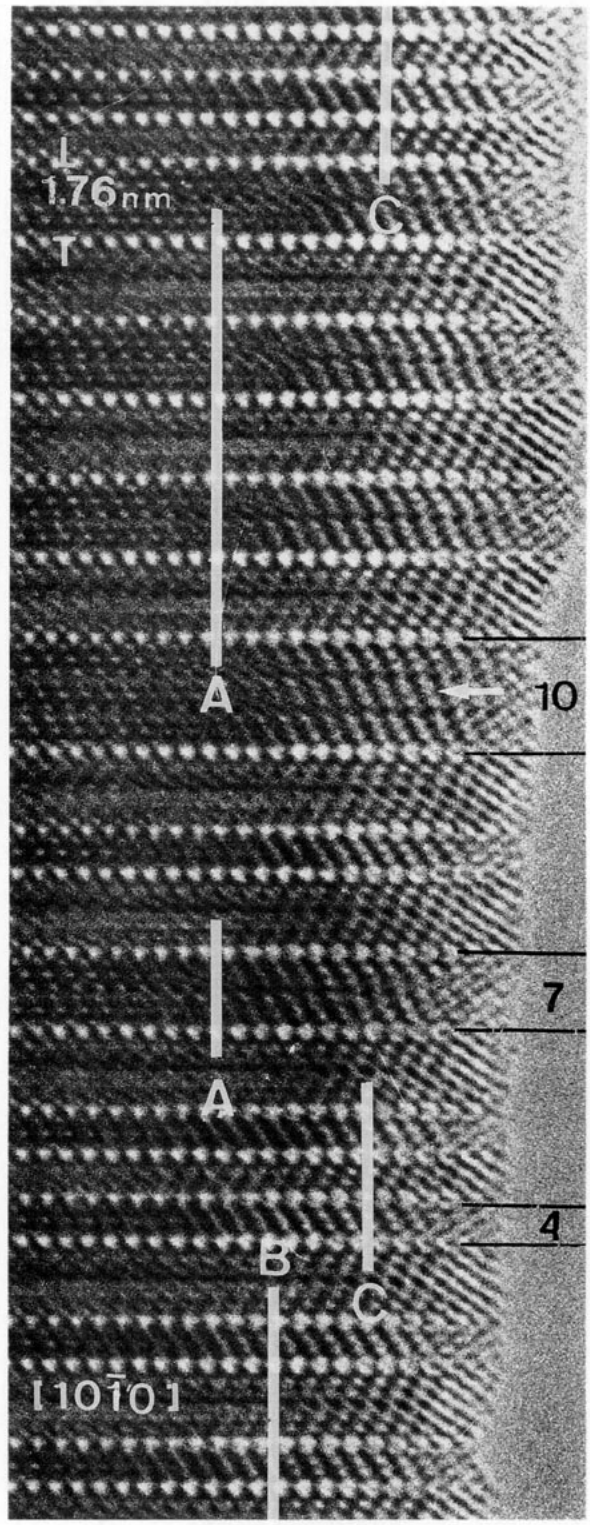

FIG. 6. HREM image of an irregular sequence of parent blocks: A indicates the ···WXW′X′··· sequence; B indicates the ···WW′X WW′X··· sequence; C indicates the ···WW′WW′··· sequence; and the arrow indicates the ···XXX··· sequence.

sity distribution along the $h\bar{h}0l$ rows with $h = 1$ and $h = 2$. The spots in the vicinity of the diagonals of the rectangle formed by the indicated intense spots with $l = 14$ are relatively the most intense ones.

6. HIGH-RESOLUTION IMAGES

The most relevant imaging zone is the one parallel to the –Ba–O–Ba–O– close-packed rows; it reveals directly the stacking sequence of the close-packed BaO_3 layers. The image of a rather irregular sequence exhibiting three different block sizes limited by an extra bright line is reproduced in Fig. 6.

Usually the imaging code is found by comparing observed and computed images. However, even without such a comparison, the characteristic geometrical features of the images can be related unambiguously to structural features of the blocks in the present case.

The rows of extra bright dots in Fig. 6, parallel to the traces of (0001) planes, are lines of symmetry; they mark the BaO layers which are situated in mirror planes of the Ba_2ScAlO_5-type lamellae. This is represented schematically in Fig. 1b.

These twin lines in Fig. 6 separate bands of three different widths. These bands consist of long dot rows parallel

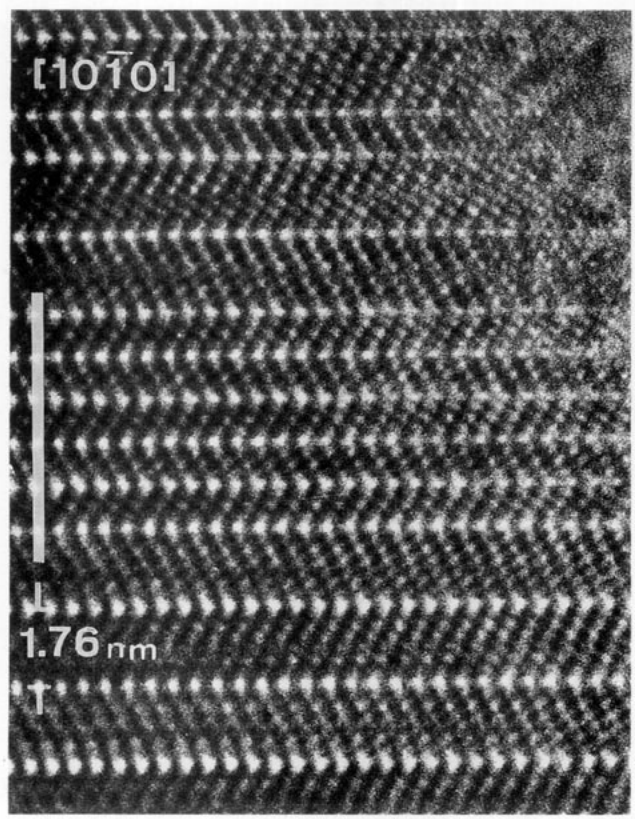

FIG. 7. HREM image illustrating a large sequence of W-type blocks.

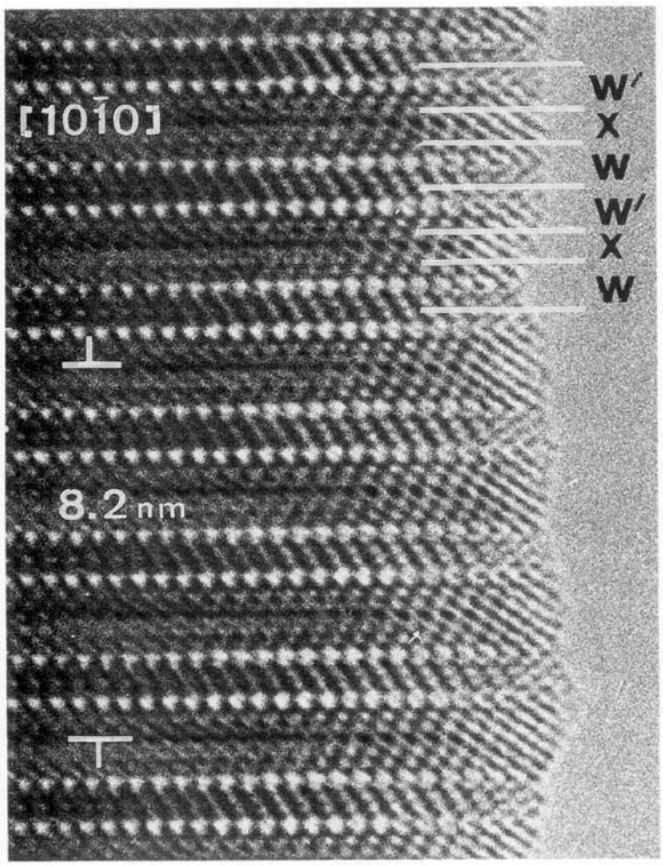

FIG. 8. HREM image illustrating a regular sequence of ···WW'X WW'X··· blocks. The lattice constant of the rhombohedral cell is shown.

to the twin lines. The same dots also form finite sequences along oblique lines in such a way that a lattice with parallelogram-shaped meshes results. Only O–Ba–O rows produce visible dots. The numbers of long dot rows in the three types of bands are respectively 4 for the narrow bands, 7 in the bands of intermediate width, and 10 in the widest bands.

It is further noted that in the seven-row band the short dot sequences, on both sides of the central row, are not aligned; there is a discontinuity in the inclined rows. This discontinuity marks the vertical stacking of two BaO_3 layers forming the layer of trigonal prismatic interstices occupied by Sc.

The broadest bands contain 10 rows of dots, and the inclined sequences exhibit two lines of discontinuity, corresponding to the two layers of trigonal prisms. The relative widths of the three types of bands observed in Fig. 6 are 4 : 7 : 10, in accordance with the models for these bands. Short periodic sequences containing bands with different widths of 4 and 7 dot rows wide have been observed.

Figure 7 reproduces the sequence with the shortest period, which consists only of bands with four dot rows. The underlying structure can be represented by the block sequence ···/WW'/WW'/···; its corresponding chemical composition is $Ba_4Sc_2Al_2O_4$ (i.e., $2 \times \beta$-Ba_2ScAlO_5). Its lattice is hexagonal with $c_H = 19.44$ Å.

The most frequently occurring block sequence in the sample under study is visible in Fig. 8. The image exhibits an alternation of narrow and wide bands. The narrow band again contains four long rows of dots, whereas the wider ones contain seven such rows. The stacking can be represented by the block sequence ···/W'WXW'WX/

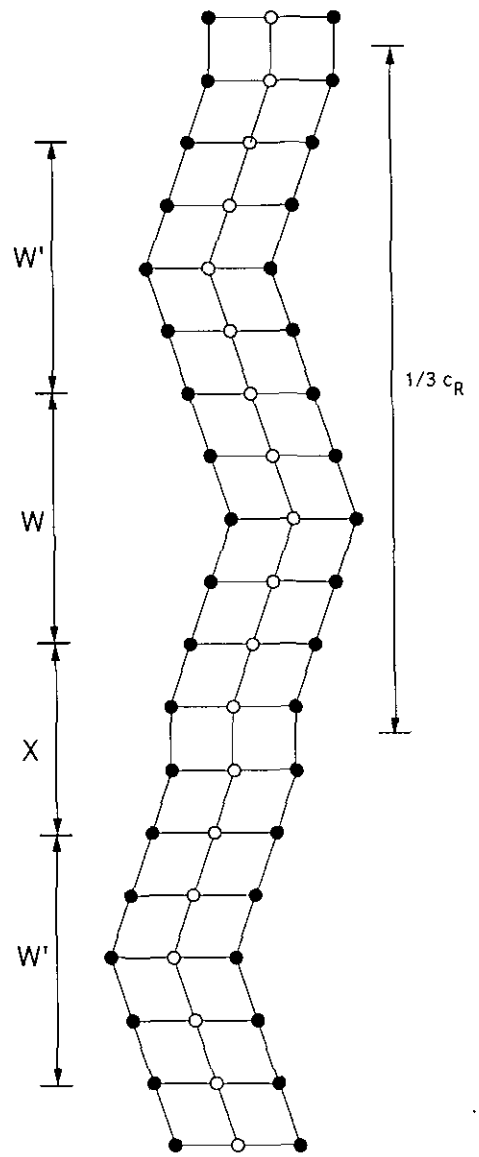

FIG. 9. Schematic representation of the ···WW'XWW'X··· block sequence.

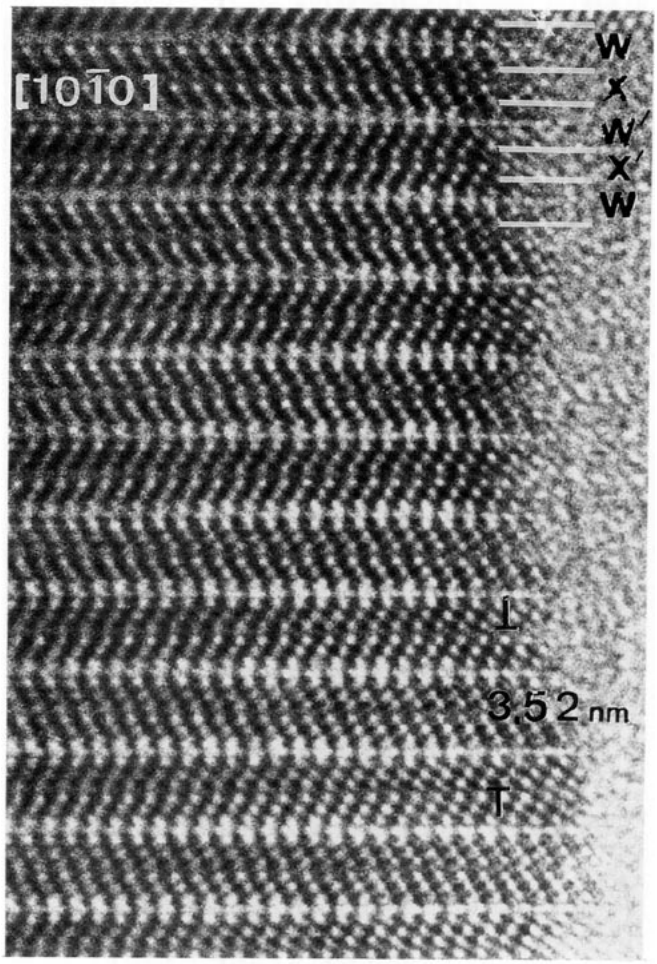

FIG. 10. HREM image illustrating a regular sequence of $\cdots$WXW'X'$\cdots$ blocks. The lattice constant of the hexagonal cell is shown.

$\cdots$; it leads to the chemical composition $Ba_{11}Sc_8Al_4O_{29}$. Figure 9 gives a schematic representation of this sequence. The widest bands have a width equal to that of XW, whereas the narrow ones have a width equal to that of a W block. The resulting c_R parameter is 82 Å in a hexagonal description, but the structure is actually rhombohedral.

An extensive sequence consisting of the regular alternation of the above described 7 row bands, in twin relation, is reproduced in Fig. 10. In terms of blocks the sequence can be represented as $\cdots$/WXW'X'/$\cdots$. The corresponding chemical composition is then $Ba_7Sc_6Al_2O_{19}$. The structure is hexagonal with c_H = 35.17 Å. In each of the X blocks the singularity along the central line reveals the BaO layers.

The interpretation of the high-resolution images, based on geometrical features, is confirmed by computer-simulated images using the "Mac Tempas" software package. Figure 11 reproduces a matrix of simulated images of the compound $Ba_7Sc_6Al_2O_{19}$ as viewed along the close-packed rows, for different thicknesses and defocus values. As assumed before, the bright lines are found to coincide with the traces of the BaO layers: they are twin lines for the dot pattern. The discontinuities in the inclined rows of dots, along the centers of the twin bands, correspond with the layers of trigonal prisms, in agreement with the interpretation.

7. DISCUSSION

Thus far we have described the different structures in terms of structural fragments of simpler structures. However, long period structures can often also be described as resulting from a simpler structure by the periodic insertion of planar interfaces. These interfaces can be of two essentially different types, either translation interfaces or coherent twin interfaces.

The system of hexagonal perovskites $La_nTi_{n-\delta}O_{3n}$ (9) provides an example of long period structures due to the periodic occurrence of intrinsic stacking faults, i.e., translation interfaces in a cubically stacked LaO_3 framework. The stacking faults are stabilized by layers of cation vacancies occupying the central layers of the triplet lamellae of face-sharing octahedra associated with the stacking faults.

The product phase resulting from the martensitic transformation in nonstoichiometric Ni–Mn (24) and Ni–Al (25) exhibits long period structures due to coherent periodic twinning on close-packed planes.

We will show that the intergrowth structures discussed above can also be interpreted as being interface modulated. The two types of interfaces occur sequentially in a cubically stacked framework of BaO_3 layers, the twins as well as the translation interfaces being stabilized by cations: the first by two layers of Al in tetrahedral coordination, and the second by layers of Sc in trigonal prismatic coordination.

We first illustrate how the $Ba_3Sc_4O_9$ structure can formally be described in terms of periodic faults generated in a cubic stacking of close-packed layers $\cdots$ABCABC$\cdots$. The displacement described by the vector $\pm\frac{1}{3}$ [10$\bar{1}$0] of one BaO_3 layer with respect to the adjacent one in an ABC sequence leads to an intrinsic stacking fault for one sense of the vector but to a vertical stacking, i.e., to A on A stacking, for a displacement in the opposite sense. Of course, the latter faults are not stable and they can only exist if the trigonal prismatic interstices so created are filled by Sc ions. The formation of the stacking sequence present in the BaO_3 framework of $Ba_3Sc_4O_9$ can be represented schematically in terms of successive shifts of cubic lamellae:

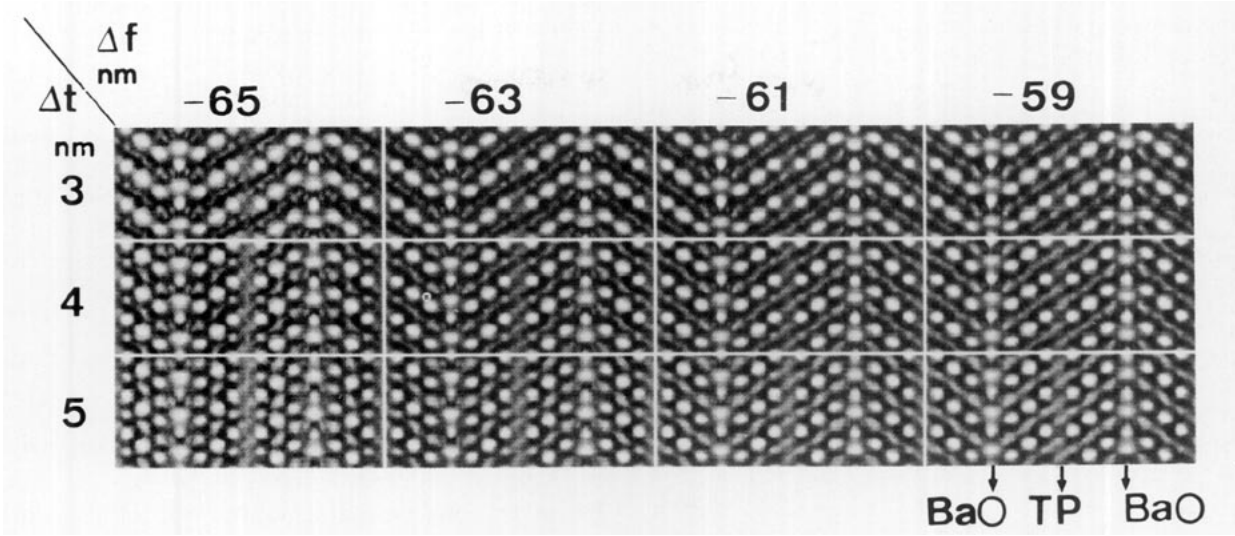

FIG. 11. Simulated high-resolution images of the $Ba_7Sc_6Al_2O_{19}$ compound along the $[10\bar{1}0]$ zone for different defocus values (horizontal) and thicknesses (vertical). The BaO rows and the trigonal prismatic (TP) interstices occupied by Sc are indicated.

A B C A B C A B C A B C
↓ ↓ ↓ ↓ ↓ ↓ ↓ ↓ ↓
A B C C A B C A B C A B
↓ ↓ ↓ ↓ ↓ ↓
A B C C A B B C A B C A
↓ ↓ ↓
A B C C A B B C A|A B C

The rearrangement of the cubic $\cdots ABC \cdots$ stacking into its twinned variant $\cdots CBA \cdots$ is well-known and needs no comments.

In summary the present system of compounds provides us with the first example of long period structures in which the long period can be related to the sequential occurrence of planar interfaces of two different types: high-energy stacking faults and coherent twin interfaces. Both types of interfaces are nonconservative; i.e., composition changes are associated with their presence, which implies that the stacking sequences are composition driven. Ideally, for each composition of the type $q \times Ba_3Sc_4O_9 + p \times Ba_4Sc_2Al_2O_{10}$ there corresponds a long period structure. For a complicated ratio $p:q$ the theoretical period may be very long. However, it should be noted that a strict period will only be found for simple ratios $p:q$, which do not lead to excessively long periods. In the latter case irregular sequences are found instead.

CONCLUSIONS

The electron microscopic study of the compound $Ba_7Sc_6Al_2O_{19}$ resulted in the discovery of a series of homologous intergrowth structures, based on periodic sequences of two building blocks consisting of structural fragments of β-Ba_2ScAlO_5 and $Ba_3Sc_4O_9$. We represent the first block by W and the second by X. The lamellae related to these by a 180° rotation about the c-axis are represented respectively by W′ and X′. The title compound can then be represented by the stacking symbol $\cdots WXW'X' \cdots$. Further stacking sequences were revealed by means of electron diffraction and high-resolution electron microscopy: $\cdots WW'WW' \cdots$, $\cdots XXX \cdots$ (or $X'X'X'$), $\cdots WW'XWW'X \cdots$, and $\cdots WXXW'X'X' \cdots$. These phases can also be considered as interface modulated structures derived from the close-packed 3R structure consisting of BaO_3 layers, the interfaces, which are coherent twins and stacking faults, being stabilized by B cations.

ACKNOWLEDGMENTS

This text presents research results of the Belgian Program on Interuniversity Poles of Attraction initiated by the Belgian State, Prime Ministers Office of Science Policy Programming. The authors assume all responsibility for the scientific content.

REFERENCES

1. J. Van Landuyt, S. Amelinckx, J. A. Kohn, and D. W. Eckart, *J. Solid State Chem.* **9,** 103 (1974).
2. S. Kuypers, G. Van Tendeloo, J. Van Landuyt, S. Amelinckx, H. W. Shu, S. Tanlmes, J. Flahant, and P. Lornelle, *J. Solid State Chem.* **73,** 192 (1988).
3. H. Maeda, Y. Tanaka, M. Eukutomi, and T. Asano, *Jpn. J. Appl. Phys. Lett.* **27,** L209 (1988).
4. H. W. Zandbergen, Y. K. Huang, M. J. V. Menovsky, G. Van Tendeloo, and S. Amelinckx, *Nature* **332,** 620 (1988).
5. G. Van Tendeloo, H. W. Zandbergen, J. Van Landuyt, and S. Amelinckx, *Appl. Phys. A* **46,** 153 (1988).

6. Z. Z. Sheng and A. H. Hermann, *Nature* **332,** 55 (1988).
7. M. Verwerft, G. Van Tendeloo, and S. Amelinckx, *Physica C* **156,** 607 (1988).
8. W. W. Jackson and J. West, *Z. Kristallogr.* **76,** 211 (1931).
9. G. Van Tendeloo, S. Amelinckx, D. Darriet, R. Bontchev, J. Darriet, and F. Weill, *J. Solid State Chem.* **108,** 336 (1994).
10. M. German and L. M. Kovba, *Russ. J. Inorg. Chem.* **28,** 2377 (1980).
11. H. J. Rother, S. Kemmler-Sack, U. Treiber, and W. R. Cyris, *Z. Anorg. Allg. Chem.* **466,** 131 (1980).
12. S. Kemmler-Sack, *Z. Anorg. Allg. Chem.* **461,** 146 (1980).
13. S. Kuypers, G. Van Tendeloo, J. Van Landuyt, and S. Amelinckx, *Acta Crystallogr. Sect. A* **45,** 291 (1989).
14. R. V. Shpanchenko, E. V. Antipov, M. V. Paromova, and L. M. Kovba, *Russ. J. Inorg. Chem. Engl. Transl.* **36,** 797 (1991).
15. R. V. Shpanchenko, E. V. Antipov, L. N. Lykova, and L. M. Kovba, *Vestn. Mosk. Univ. Ser. Khim.* **31,** 555 (1990).
16. L. M. Kovba and M. V. Paromova, *Vestn. Mosk. Univ. Ser. Khim.* **21,** 621 (1970).
17. Hk. Müller-Buschbaum and M. Abed, *Z. Anorg. Allg. Chem. B* **591,** 174 (1990).
18. P. B. Frit, B. Holmberg, and J. Galy, *Acta Crystallogr. Sect. B* **26,** 16 (1970).
19. Hk. Müller-Buschbaum and O. Schrandt, *J. Alloys Compounds* **191,** 151 (1993).
20. G. Van Tendeloo, B. Van Dyck, S. Kuypers, and S. Amelinckx, *Phys. Status Solidi A* **101,** 339 (1987).
21. G. Van Tendeloo, D. Van Dyck, S. Kuypers, H. W. Zandbergen and S. Amelinckx, *Phys. Status Solid: A* **102,** 597 (1987).
22. D. Van Dyck, D. Colaitis, and S. Amelinckx, *Phys. Status Solidi A* **68,** 385 (1981).
23. D. Colaitis, D. Van Dyck, and S. Amelinckx, *Phys. Status Solidi A* **68,** 419 (1981).
24. I. Baele, G. Van Tendeloo, and S. Amelinckx, *Acta Metall.* **35**(2), 401 (1987).
25. D. Schryvers, *Phil. Mag. A* **68,** 1017 (1993).